MATERIALS SCIENCE & ENGINEERING B

ELSEVIER

Materials Science and Engineering B43 (1997) 185–191

Dynamics of excited states in GaN

A. Hoffmann*

Institut für Festkörperphysik der TU Berlin, Hardenbergstr. 36, 10623 Berlin, Germany

Abstract

We report a review of the optical properties of GaN epilayers. Photoluminescence, time-resolved and photoluminescence excitation measurements on hexagonal and cubic GaN heterostructures from the band edge region down to the near infrared spectral region provide information about excitonic properties as well as the influence of point and extended defects. Spatially resolved Raman-scattering and photoluminescence experiments allow to analyze the crystal structure, layer orientation and strain contribution to the lattice properties. Luminescence measurements at high excitation densities will be presented giving information about optical gain mechanisms. © 1997 Elsevier Science S.A.

Keywords: GaN epilayers; Photoluminescence; Optical gain mechanism

1. Introduction

Short wavelength or visible light emitting-(LED) and laser-diodes certainly have applications in communications, displays, high density optical storage systems, traffic signals and many other spheres of life. High-brightness semiconductor LEDs manufactured from multi-quantum well structures of III–V nitrides [1] have large quantum efficiencies and emit in the blue, green and yellow spectral region, which allows fabrication of flat, full color visual displays. Recently, the first laser diode based on an InGaN heterostructure has been achieved by the Nichia company [2]. This demonstrates the great progress made in the field of GaN research.

In spite of this recent success in device techniques [3], some of the basic electrical and optical properties of III–V nitrides are still unknown [4]. This is often a problem of the material quality and a lack of a better understanding of the epitaxial growth techniques. The purpose of the paper is to present the state of the art in the investigation of optical recombinations in GaN epilayers with emphasis on the dynamics.

2. Samples and experimental

The investigated bulk-like sample with a thickness of 400 μm was grown by hydride vapor phase epitaxy (HVPE) without any buffer layer. The metal organic vapor phase epitaxy (MOVPE) epilayers of thickness around 3 μm were deposited on a 35 nm AlN buffer. All these samples were hexagonal and were grown on sapphire substrates. The electron concentrations of the layers determined by CV measurements are around 10^{17} cm^{-3} at room temperature. The cubic GaN epilayers were grown on GaAs substrates by molecular beam epitaxy (MBE). The thickness of these GaN films were less than 1 μm.

PL was excited for the steady state experiments by the 325 nm line of a HeCd laser and time-resolved measurements were performed at various temperatures using a frequency-doubled dye laser synchronously pumped by an actively mode-locked and frequency-doubled Nd:YAG laser. The overall time resolution employing convolution techniques was 15 ps. The PLE measurements and the two-color stimulation experiments were done with either a monochromator/tungsten lamp combination as tunable light source or different laser lines of a semiconductor laser and an Ar-ion laser. In a calorimetric absorption spectroscopy (CAS) experiment in the mK range [5] we measured the temperature increase of the photo-excited sample as a function of excitation energy. It is effected by the generation of phonons during nonradiative relaxation

* Corresponding athor. Tel. +49 30 31422001; fax: +49 30 31422064; e-mail: axel0431@mailszrz.zrz.tu-berlin.de

0921-5107/97/$17.00 © 1997 Elsevier Science S.A. All rights reserved.
PII S0921-5107(96)01860-0

to thermal equilibrium. In a calorimetric reflectivity spectroscopy (CRS) experiment the reflection of the sample was detected by the absorption-induced heating of a black body. CAS and CRS spectra were recorded simultaneously. We used an excimer-laser-pumped dye laser as monochromatic light source giving a spectral resolution of 50 μeV. Raman-scattering experiments (resolution 2 cm^{-1}) were excited with the 632.8 nm line of a HeNe laser or different lines of an Ar-ion laser. The scattered light was detected in backscattering geometry and analyzed by a Dilor LABRAM single-grating spectrometer with a charge-coupled device (CCD) detector.

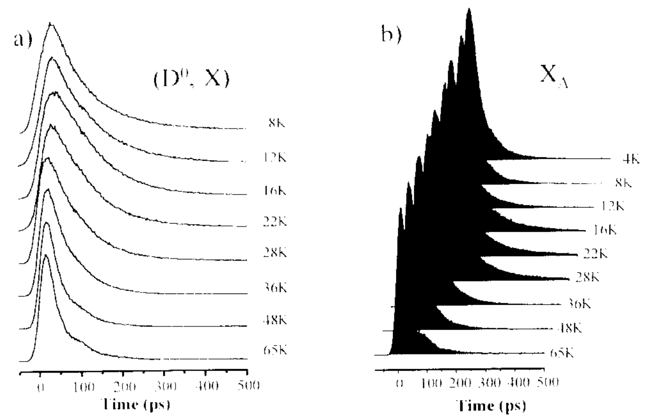

Fig. 2. Luminescence transients (a) from donor-bound exciton (D^0, X), (b) from the free A-exciton X_A, taken at different lattice temperatures after excitation from the GaN epilayer side.

3. Results

In Fig. 1 a luminescence overview of typical optical transitions in a hexagonal GaN epilayer at 1.8 K is shown. The energy range around 3.48 eV (right spectrum) represents the emission lines of the free and bound excitons in GaN, the spectrum in the middle exhibits the donor–acceptor-pair (DAP) and the yellow luminescence, while in the left spectrum different emission lines of internal transitions of unintentionally doped transition metal ions are shown. In the following all of these different luminescence lines will be discussed. Special interest was focused on the dynamical behavior of these recombination because it is one of the most sensitive methods to investigate radiative and nonradiative properties.

3.1. Exciton dynamics

The right luminescence spectrum of Fig. 1 shows that free and donor-bound excitons contribute to strong radiative recombination in high-quality GaN at low temperatures. To get a better picture of the influence of nonradiative processes it is necessary to increase the temperature. We observed a rapid decrease of the intensity of the donor-bound exciton with raised temperatures governed by an activation energy of 7 meV. This value agrees very well with the localization energy of the exciton at the shallow donor. The physical process involved is the dissociation of the exciton from the donor caused by the absorption of low-energy acoustical phonons which are present even at relatively low temperatures. We will now show that this process also governs the recombination dynamics of the donor-bound exciton (see also [6]). In Fig. 2(a) luminescence transients of the shallow-donor-bound exciton line after band-to-band excitation are shown for different values of the lattice temperature. 'Bumps' in the very fast transients are caused by the response of our detection system to ps-signals and do not have any physical meaning. No rise process can be resolved in any transient. From this we have to conclude that the lifetime of the free exciton is shorter than our time resolution of 15 ps at low temperatures. The lifetime of the donor-bound exciton of 70 ps at 8 K is seen to decrease continuously with increasing temperature, reproducing well the expected increased dissociation rate as was also reported by Chen et al. [7]. How does this increased dissociation affect the transients of the free exciton? The answer is given in Fig. 2(b). At low temperatures the decay is fast as expected from the lack of a rise process in the bound-exciton transients. As soon as the donor-bound exciton decay becomes faster with increasing temperature, the luminescence transient of the free exciton slows down. Above 28 K the faster free exciton returns.

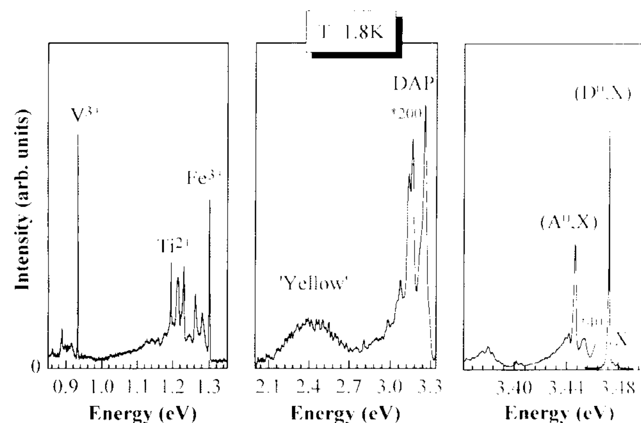

Fig. 1. Overview luminescence spectra of a hexagonal GaN HVPE sample at 1.8 K. The crystal is excited at 3.81 eV (right and middle spectrum) and at 2.6 eV (left spectrum).

To prove that the dissociation of the bound-exciton from the donor is responsible for this temperature dependence of the free-exciton transient, we evaluated a three-level model with temperature-dependent transition probabilities, Fig. 3(a). Corresponding to our ex-

perimental excitation conditions we assume the system to be in the free-exciton state initially. Here, we neglect the comparatively short exciton formation time. We also assume that the only temperature-dependent process is the thermally activated dissociation of the bound exciton from the donor, given by the characteristic time constant τ_{23} , cf. Fig. 3(a). Its temperature dependence is set as

$$\tau_{23} = \tau'_{23} \exp(\Delta E/kT) \quad (1)$$

ΔE denotes the localization energy of the exciton at the shallow donor, k Boltzmann's constant and T the lattice temperature. The decay rate of the free exciton is assumed to be independent of the lattice temperature. The solution from the two coupled rate equations was used to model luminescence transients by convolution with the response of our detection system to the laser pulse, see Fig. 3(b). The effects observed in the experiment are nicely reproduced by the calculated transients even though a perfect fit has not been achieved. We ascribe the difference between the measured and calculated transients to the effect of the second donor-bound exciton with 3.6 meV localization energy. However, the parameters used in the calculation of the transients, which give the closest resemblance to the observed temperature behavior, are shown in Fig. 3(b) and serve as a reasonable estimate of the actual transition times. We see that not only the decay time τ_{31} describing the annihilation of the exciton is short in comparison with free exciton lifetimes in other high-quality materials such as CdS, but also that there is a strong influence of the shallow donors which capture free excitons at low temperatures within 1 ps.

To summarize dynamic results on free and shallow bound excitons in structurally relaxed regions of GaN, through an analysis of the temperature dependence of

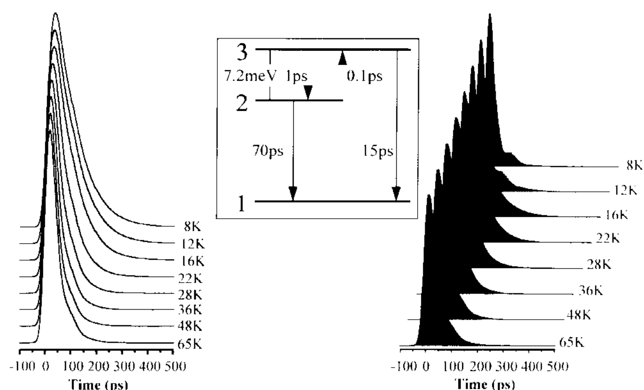

Fig. 3. (a) Three-level system used to model the energy relaxation dynamics of free (level 3) and shallow (2). Dotted arrows denote radiationless processes. (b) Calculated luminescence transients of free exciton obtained from the model of Fig. 3(a) using the parameters shown. The temperature dependence of the measured transients shown in Fig. 2 (b) is qualitatively reproduced.

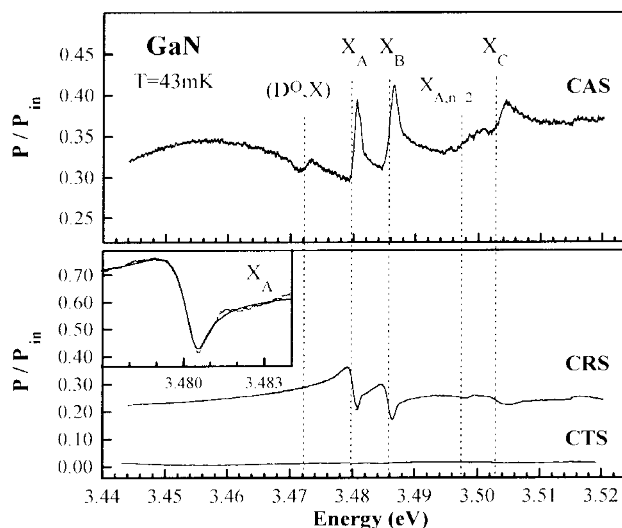

Fig. 4. Calorimetric absorption (CAS), calorimetric transmission (CTS) and calorimetric reflection (CRS) spectra of GaN. In the inset the reflection curve of the A-exciton is fitted in a polariton model.

the luminescence transients we obtained an estimate of the time constants governing the energy relaxation in this energy range. We observe a fast luminescence decay of the free exciton which is additionally accelerated at low temperatures by the capture at the shallow donor. Further nonradiative relaxation processes have to be taken into consideration to account for the short exciton decay time τ_{31} of less than 15 ps. The observation of transition metals (left spectrum of Fig. 1) in this sample which are known to act as 'luminescence killers' is a likely explanation.

To quantify the nonradiative processes we have an efficient tool to measure directly the heating of the sample by a calorimetric method in the mK range. The received calorimetric signals can be calibrated through an external electrical heater, so that we measure absolute values given in Watts. In Fig. 4 highly resolved calorimetric absorption (CAS), calorimetric transmission (CTS) and calorimetric reflection (CRS) of a 400 μm GaN/Al_2O_3 epilayer are shown (see also [8]). Three structures are clearly resolved in the CRS spectrum and attributed to the excitons FX(A) at 3.4800 eV, FX(B) at 3.4806 eV and FX(C) at 3.5025 eV, involving holes from the A-, B,- and C-valence-bands, respectively. The energy differences of these values represent the splitting of the three valence bands of a strain-free GaN epilayer. A minor structure is detected at 3.4995 eV and ascribed to the FX(A) $n = 2$ exciton and, hence, gives 26.1 meV for the free binding energy. Since the reduction of the reflectivity implies an increase of light absorption in the crystal, which in turn triggers nonradiative processes, the same fine structures as in CRS are also seen in the CAS. Additional structure in the CAS appears as a dip at 3.4727 eV. It is caused by the

neutral-donor-bound-exciton absorption in transmission (the transmission coefficient is nearly zero in the range). Thus, the calorimetric detection of the donor-bound-exciton absorption demonstrates the advantage and high sensitivity of the CAS technique. The decrease of the CAS signal at the spectral position of the D^0X-line implies a decrease of the phonon emission rate and, therefore, enhanced radiative relaxation. Adding up the CTS, CRS and CAS shows that in this sample the quantum efficiencies of the donor-bound exciton and of the free exciton are 50% and 25%, respectively. In the inset of Fig. 4 the reflectivity loop of the FX(A) is fitted by a pollution model. From the best fit we obtain the following parameters: the eigenfrequency ω_0 of the FX(A) is 3.480 eV, the damping constant Γ which is a direct measure of the polariton-impurity interaction is 0.65 meV showing that the quality of the crystal is reasonable good. The longitudinal tranversal splitting of the exciton ω_{LT}, which is proportional to the oscillator strength, is 0.64 meV. The background dielectric constant ε_0 is 9.7, the perpendicular components of the effective masses of the hole and the electron are $0.75m_0$ and $0.23m_0$, respectively. Although the polariton data and the halfwidth of the donor-bound exciton (0.9 meV) in this GaN sample reflects the excellent quality of crystal, the calorimetric data demonstrate that the nonradiative part of the excitonic transition probability is dominant. This is in agreement with the time-resolved experiments.

3.2. High density effects and gain investigations

The recent realization of a group III–V-nitride-based laser [2] avails urgently exploratory physical process which provides the optical gain. For a comprehensive understanding of the gain mechanisms in laser structures it is important to know the intrinsic luminescence properties of highly excited GaN. Low temperature emission spectra from a 300 μm thick GaN grown by hydride vapor phase epitaxy show under low density excitation only a sharp donor-bound exciton line I_2 at 3.478 eV with a halfwidth of 0.9 meV. Increasing the excitation density the I_2 line broadened and shifted to smaller energies (see also [9]). Since the broadened I_2 line is also to be seen for excitation densities of 50 MW cm^{-2} and the increase of this line grows superlinear with the excitation density, we attribute this line to a high density excitation process where a biexciton M recombines. The estimated binding energies were in the range between 2–3 meV. At 50 MW cm^{-2} the dominating luminescence line is the P-band at 3.456 eV which is attributed to the inelastic exciton-exciton scattering. In Fig. 5a the temperature dependence of the high-density excitation (8 MW cm^{-2}) luminescence is shown. At low temperatures the luminescence of the biexciton decay M and of the exciton–exciton collision P are the dominant features in the spectra. It is clearly seen that with increasing temperatures the contribution of phonon-assisted recombination processes to the luminescence intensity becomes larger. At intermediate temperatures the luminescence of the exciton–LO phonon scattering dominates the spectra. There are further structures which can be identified by their characteristic red shift with increasing temperature and is well known from exciton–electron scattering in other wide gap materials. At room temperatures the electron–hole plasma and the exciton-hole scattering dominating the luminescence. The corresponding gain spectra are represented in Fig. 5b for excitation densities of 8 MW cm^{-2}. The dominating gain mechanism at low temperatures is the inelastic exciton–exciton scattering. In the temperature range around 100 K gain mechanisms of the exciton–electron, of the exciton–phonon scattering become dominant. At room temperatures the dominant lasing mechanisms are probably the electron–hole plasma and the exciton–LO phonon scattering. Further detailed measurements and lineshape fits are under way to unambiguously determine the luminescence and gain properties of GaN.

3.3. Structural defects and yellow luminescence

This section will demonstrate that structural defects influence strongly the dynamics of optical transitions in GaN. Two examples will be given. First structural minority phases in GaN will be investigated [10]. Then, we will show that the dominating recombination processes near the interface between GaN and its lattice-mismatched substrate differ strongly from those far away from the interface [11], e.g., near the surface of the epilayer. We will show that in structurally perturbed regions such as in the vicinity of the interface, the

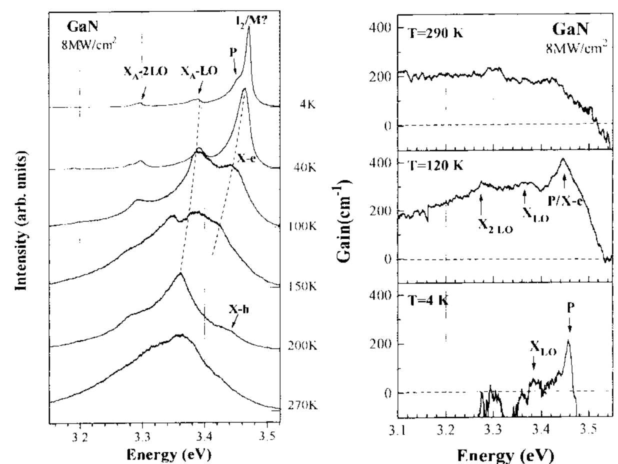

Fig. 5. (a) Temperature dependence of the high density excitation luminescence lines in GaN. The excitation density is 8 MW cm^{-2}. (b) Temperature dependence of the gain spectrum.

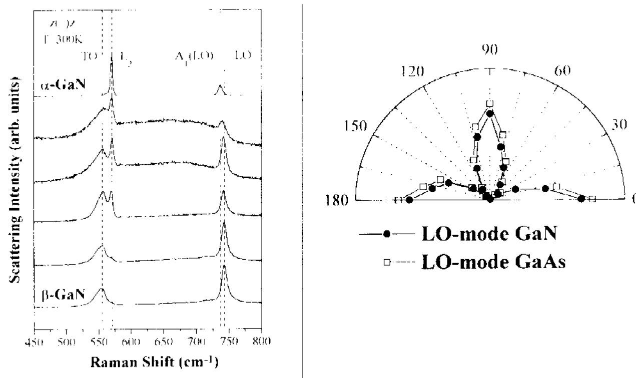

Fig. 6. Left spectra represent spatially resolved Raman spectra. On the right hand side Polarization dependence of the parallel polarized GaN and GaAs LO-phonon intensity as the sample is rotated. An angle of 45° corresponds to $z(yy)\bar{z}$.

radiative recombination of free and shallow bound excitons is quenched and deep dislocation excitons [6] and often the yellow luminescence appear in the spectrum.

If GaN grows on cubic GaAs, e.g. by MBE, the cubic modification of GaN can be observed. Cubic GaN has an energy gap which is approximately 0.22 eV [12] less than the hexagonal phase. Up to now, even the exact value of the bandgap of cubic GaN is still an object of discussion. Due to the strong mismatch between GaAs and GaN, the dislocation density near the interface is high and often one observes hexagonal minority phases. A very sensitive and straightforward tool for the quantitative determination of a structural minority phase in GaN is the Raman scattering. In Fig. 6 (left hand side) spatially resolved Raman spectra of cubic, hexagonal and mixed phases are shown in $z(\ldots)\bar{z}$ configuration. In- and on-plane excitations, as well as polarization dependent measurements on predominantly cubic and hexagonal GaN samples, were performed and forward scattering effects were found. In order to obtain quantitative information we measured the polarization dependence of the phonon modes of the cubic sample. Fig. 6 (right hand side) shows polar plots of the intensity of the LO phonon mode of GaN compared to the LO mode of GaAs. In this experiment the incident and scattered polarization were kept fixed and parallel polarized, while the sample was rotated in total by 180° in the plane defined by the polarization. The GaN mode shows the same polarization dependence as the GaAs mode indicating that the sample is grown epitaxially. If both phases coexisted in the sample, the different polarization dependencies would overlap and the distinct d-wave like minima of the scattering intensity would disappear with increasing hexagonal-phase content. From these considerations we found a cubicity of $98 \pm 2\%$. Thus, the cubic sample investigated contains at most 2% hexagonal subdomains. Furthermore, the polar plot demonstrates that GaN grows epitaxially on GaAs. The excitonic recombination of these samples is dominated by the emission at 3.26 eV which we attribute to the cubic donor-bound exciton. Assuming similar binding energies for both the cubic and hexagonal GaN we receive a band gap energy of 3.286 eV for cubic GaN.

Fig. 7 represents spatially resolved luminescence and Raman spectra of a hexagonal GaN epilayer grown on sapphire. The excitation wavelength of the laser is indicated through an arrow in the luminescence spectrum (left hand side). The figure shows a 40 μm long linescan across the GaN-substrate interface where we have taken a spectrum every 1 μm. The region of the substrate is marked by the presence of the A_g sapphire mode at 419 cm^{-1} (for a survey of Raman spectra on sapphire see, e.g., [13]). The transition to the GaN layer is indicated by the appearance of the A_1(TO) and the E_2 modes at 534 cm^{-1} and 569 cm^{-1}, respectively. A photoluminescence band with an intensity maximum at 2.4 eV appears directly at the interface with the substrate. The spatial width of the region, from which this photoluminescence occurs is about 3 μm. The GaN region is dominated by the abruptly increasing A_1(TO) mode. At a distance d of about 30 μm away from the substrate interface, in a region several μm wide, a second broad photoluminescence appears peaking at the same spectral position as the first band. Simultaneously with the increasing photoluminescence the intensity of the A_1(TO) Raman signal decreases but the mode continues to be visible. The decrease of the A_1(TO) Raman signal (near $d = 20$ μm) and the broad photoluminescence band (at $d = 30$ μm) is closely connected with a reorientation of the GaN structure caused by structural defects. This can be proven through the change in scattering intensity of the different phonon modes in dependence on the distance from the interface. While both the E_2 mode and the A_1(TO) mode appear in this region, the ratio of their intensity inverts with increasing distance from the substrate interface. The change in intensity starts where the second photo luminescence band appears. Individual Raman spectra taken at distances 15, 25 and 50 μm away from the interface show that near the interface with the substrate ($0 \leqslant d \leqslant 20$ μm) the spectra are dominated by the A_1(TO) mode, the intensity of the E_2 mode increases with the appearance of the second photoluminescence band and becomes the most intense phonon mode ($d > 35$ μm). The inversion of the relative intensities where the second band appears can be explained by a structural reorientation of the GaN layer. This indicates that the 2.4 eV luminescence is probably connected with defects present in the region of reorientation. Probable defect candidates are cation or anion vacancies. Recent calculations (J. Neugebauer, private communications). indicate the high probability of the

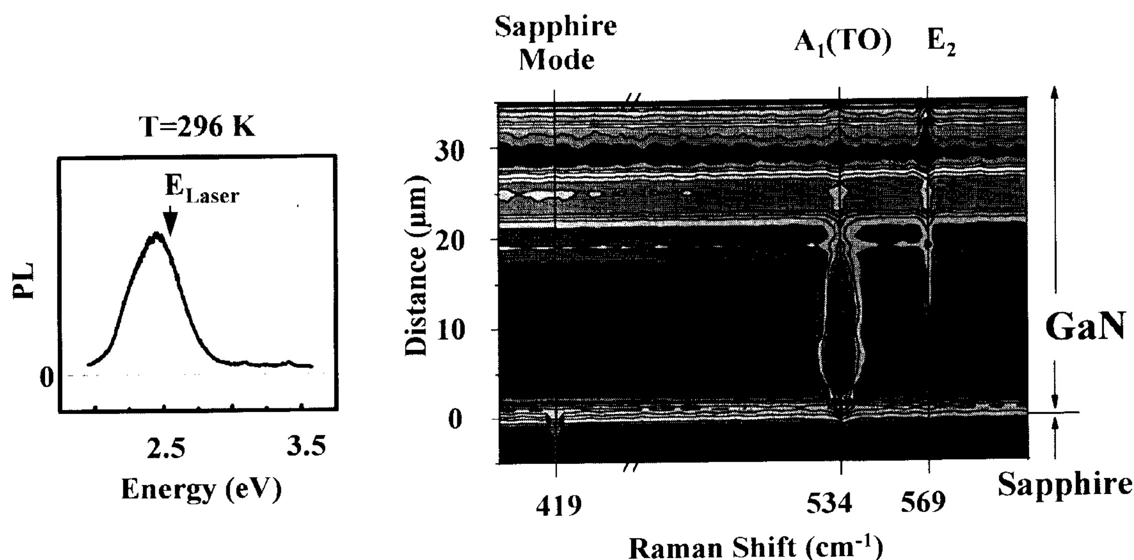

Fig. 7. Time-resolved luminescence and Raman spectra of GaN at room temperature. Left: the 2.4 eV luminescence of GaN. The arrow indicates the excitation energies of the laser used for the Raman investigations. Right: Linescan across the GaN substrate interface. The region of the sapphire substrate and the GaN layer is marked. In order to emphasize the sapphire Raman mode it was multiplied by a factor of 2.

formation of cation vacancies in the interface region. This explains the similarity between the spectroscopic properties of the A-centers in II–VI compounds and the broad 2.4 eV luminescence band. In this context the 2.4 eV band could be explained as a deep donor–acceptor- pair luminescence like recombination between shallow donors and deep cation vacancies. Assuming that the luminescence in the underground of the Raman spectra comes from the interface it is also observed in luminescence investigations. The right luminescence spectrum of Fig. 1 was obtained after excitation of the 400 µm sample on the surface of the epilayer. The donor-bound–exciton line I_2 at 3.4782 eV is most prominent. Emission from the free A-exciton is seen at 3.4800 eV but almost no yellow luminescence is observed. The reason for this is that the 325 nm laser light does not penetrate in the interface region. The spectrum obtained after excitation of the epilayer through the sapphire substrate at the same excitation density differs very much from that just described. No free and shallow-bound-exciton luminescence are observed here. Instead we see a complex structure of lines between 3.37 eV and 3.31 eV which at higher excitation densities reveals even more lines down to 3.29 eV. These lines were already observed in hexagonal epilayers on SiC [14], and also cubic samples on GaAs [10,15], all grown without buffer layer. The fact that they were observed in samples on various lattice-mismatched substrates indicates that they are an inherent property of structurally disturbed GaN. We see that here the free and shallow bound excitons decay entirely nonradiatively. We attribute the observed 'interface' emissions to the annihilation of excitons deeply bound to defect centers connected with dislocations. The excitonic character of these lines will become clear below. Dislocation excitons are well known in other materials like CdS [16,17]. Beside these dislocation excitons again the broad emission band at 2.4 eV of Fig. 1 is observed.

3.4. Transition metals

Fig. 1 shows that the intracenter recombination of transition metal (TM) elements dominates the spectral region between 0.7 eV and 1.4 eV. The TM impurity acts as minority lifetime killers and open up additional nonradiative recombination channels for excited electrons and holes leading to a decrease of near band gap emission intensity. Two-color stimulation results in [18] show that the quenching of the yellow luminescence and the stimulation of the inner Fe^{3+} luminescence results from energy transfer processes via free holes in the valence band. As yet, four TM related luminescence bands are observed. On the basis of Zeeman and ODMR investigations the 1.3 eV luminescence is unambiguously assigned to the Fe^{3+} ($^4T_1 - {}^6A_1$) transition [19,20], whereas the origin of the other three luminescence bands is still controversial. In order to clarify their chemical nature we investigated TM codoped GaN layers grown on 6H SiC. The 1.19 eV luminescence has been attributed to the $^1E - {}^3A_2$ Transition of either Cr^{4+} [21] or Ti^{2+} [22]. We observe the luminescence only in Ti doped crystals whereas no signal could be detected in the Cr doped sample. For the remaining two luminescence bands no codoping influence is observed and the assignment to Co^{2+}/Ni^{3+} (1.047 eV) and V^{3+} (0.931 eV) remains tentative. Often in the

literature the attribution of impurities is done by an internal reference rule of Langer and Heinrich [23], e.g., comparing TM excitation spectra of GaN and GaAs. Recent photoluminescence excitation investigation of Fe^{3+} [24] show that the deep Fe^{2+}/Fe^{3+} acceptor level is found 3.17 eV above the valence band minimum makes this internal reference rule not applicable to GaN/GaAs heterostructure.

4. Conclusions

In conclusion, we investigated the optical properties of GaN epilayers with different optical methods. It is shown that the crystal quality of GaN epilayers is tremendously improved (see, e.g., the polariton data of Fig. 4). Nevertheless, our dynamical investigations show that the excitonic decay is strongly influenced by dislocations, interface defects and deep centers. This demands for further efforts in the future.

Acknowledgements

This work was partly supported by Deutsche Forschungsgemeinschaft. L. Eckey, H. Siegle, P. Thurian, R. Heitz, P. Maxim, and J. Holst made the success of the project possible by their dedicated work. The author is very grateful to several growth teams for providing us with specimens: T. Detchprohm and K. Hiramatsu (Nagoya University, H. Amano and I. Akasaki (Meijo University), D. Schikora and K. Lischka (Universität Paderborn), S. Fischer and B.K. Meyer (TU München).

References

[1] S. Nakamura, M. Senoh, N. Nawasa and S. Nagahama, *Jpn. J. Appl. Phys. Lett.*, *34* (1995) L797.
[2] S. Nakamura, in A. Yoshikawa, K. Kihino, M. Kobayashi and T. Yasuda (Eds.), *Proc. Int. Symposium on Blue Laser and Light Emmitting Diodes*, Chiba University, Japan, March 1996, p. 119.
[3] S.N. Mohammad, Arnel A. Salvador and Hadis Morkoc, *Proc. IEEE*, *83* (1995) 1306.
[4] B. Monemar, J.P. Bergman, H. Amano, T. Detchprohm, K. Hiramatsu and H. Sawaki, in A. Yoshikawa, K. Kihino, M. Kobayashi and T. Yasuda (Eds.), *Proc. Int. Symposium on Blue Laser and Light Emitting Diodes*, Chiba University, Japan, March 1996, p. 135.
[5] L. Podlowski, A. Hoffmann and I. Broser, *J. Cryst. Growth*, *117* (1992) 698.
[6] L. Eckey, A. Hoffmann, R. Heitz, I. Broser, B.K. Meyer, T. Detchprohm, K. Hiramatsu, H. Amano and I. Akasaki, *Proc. MRS Fall Meeting*, Boston, 1995.
[7] G.D. Chen, M. Smith, J.Y. Lin, H.X. Jiang, M. Asif Kahn and C.J. Sun, *Appl. Phys. Lett.*, *67* (1995) 1653.
[8] L. Eckey, L. Podlowski, A. Göldner, A. Hoffmann, I. Broser, B.K. Meyer, D. Volm, T. Streibl, T. Detchprohm, K. Hiramatsu, H. Amano and I. Akasaki, *Proc. Int. Conf SiC and Related Materials*, Kyoto, Japan, 1995, IOP Publishing, to be published.
[9] L. Eckey, J. Holst, A. Hoffmann, I. Broser, T. Detchprohm and K. Hiramatsu, *Proc. 1st Int. European Workshop on GaN*, Rigi (CH), 1996.
[10] H. Siegle, L. Eckey, A. Hoffmann, C. Thomsen, B.K. Meyer, D. Schikora, M. Hankeln and K. Lischka, *Solid State Commun.*, *96* (1995) 943.
[11] H. Siegle, P. Thurian, L. Eckey, A. Hoffmann, C. Thomsen, B.K. Meyer, H. Amano, I. Akasaki, T. Detchprohm and K. Hiramatsu, *Appl. Phys. Lett.*, *68* (1996) 1265.
[12] P. Thurian, L. Eckey, H. Siegle, J. Holst, P. Maxim, R. Heitz, A. Hoffmann, Ch. Thomsen, I. Broser, K. Pressel, I. Akasaki, H. Amano, K. Hiramatsu, T. Detechprohm, D. Schikora, M. Hankeln and K. Lischka, in A. Yoshikawa, K. Kihino, M. Kobayashi and T. Yasuda (Eds.), *Proc. Int. Symposium on Blue Laser and Light Emmitting Diodes*, Chiba University, Japan, March 1996, p. 180.
[13] S.P.S. Porto and R.S. Krishan, *J. Chem. Phys. Rev.*, *47* (1967) 1009.
[14] L. Eckey, J.-Ch. Holst, P. Maxim, R. Heitz, A. Hoffmann, I. Broser, B.K. Meyer, C. Wetzel, E.N. Mokhov and P.G. Baranov, *Appl. Phys. Lett.*, *00* (1996) 000.
[15] C.H. Hong, D. Pavilidis, S.W. Brown and S.C. Rand, *J. Appl. Phys.*, *77* (1995) 1705.
[16] J. Gutowski and A. Hoffmann, *Mater. Sci. Forum*, *38–41* (1989) 1391–1396.
[17] A. Hoffmann, J. Christen and J. Gutowski, *Advanced Materials for Optics and Electronics 1* (1992) 25.
[18] A. Hoffmann, L. Eckey, P. Maxim, J.-Chr. Holst, R. Heitz, D.M. Hoffmann, D. Kovalev, G. Steude, D. Volm, B.K. Meyer, T. Detechprohm, H. Amano and I. Akasaki, Proc. Topical Workshop on III–V Nitrides, TWN '95, Nagoya, *Solid State Electron.*, *00* (1995) 000.
[19] K. Maier, M. Kunzer, U. Kaufmann, J. Schneider, B. Monemar, I. Akasaki and H. Amano, *Mater. Sci. Forum*, *143–147* (1994) 93.
[20] R. Heitz, P. Thurian, I. Loa, L. Eckey, A. Hoffmann, I. Broser, K. Pressel, B.K. Meyer and E.N. Mokhov, *Appl. Phys. Lett.*, *67* (1995) 2822.
[21] J. Baur, U. Kaufmann, M. Kunzer, J. Schneider, H. Amano, I. Akasaki, T. Detechprohm and K. Hiramatsu, *Appl. Phys. Lett.*, *64* (1994) 857.
[22] R. Heitz, K. Pressel, P. Thurian, I. Loa, L. Eckey, A. Hoffmann, I. Broser, B.K. Meyer and E.N. Mokhov, *Phys. Rev.*, *B52* (1995) 16508.
[23] J.M. Langer and H. Heinrich, *Phys. Rev. Lett.*, *55* (1985) 1414.
[24] R. Heitz, P. Maxim, L. Eckey, P. Thurian, I. Broser, K. Pressel and B.K. Meyer, submitted to *Phys. Rev.*